

35 **Abstract.**

36 We present the first gridded and temporally continuous quantitative pollen-based plant-cover reconstruction for
37 temperate and northern sub-tropical China over the Holocene (11.7 ka BP to present) applying the Regional
38 Estimates of Vegetation Abundance from Large Sites (REVEALS) model. The objective is to provide a dataset of
39 pollen-based land cover for the last ca. twelve millennia suitable for palaeoclimate modeling and evaluation of
40 simulated past vegetation cover from dynamic vegetation models and anthropogenic land-cover change (ALCC)
41 scenarios. The REVEALS reconstruction was achieved using 94 selected pollen records from lakes and bogs at a
42 $1^{\circ}\times 1^{\circ}$ spatial scale and a temporal resolution of 500 years between 11.7 and 0.7 ka BP, and three recent time
43 windows (0.7–0.35 ka BP, 0.35–0.1 ka BP, and 0.1 ka BP–present). The dataset includes REVEALS estimates of
44 cover and their standard errors (SEs) for 27 plant taxa in 75 $1^{\circ}\times 1^{\circ}$ grid cells distributed within the study region.
45 The 27 plant taxa were also grouped into six plant functional types and three land-cover types (coniferous trees
46 CT, broadleaved trees BT, and C3 herbs C3H/open land OL), and their REVEALS estimates of cover and related
47 SEs were calculated. We describe the protocol used for the selection of pollen records and the REVEALS
48 application (with parameter setting), and explain the major rationales behind the protocol. As an illustration we
49 present, for eight selected time windows, gridded maps of the pollen-based REVEALS estimates of cover for the
50 three land-cover types (CT, BT, and C3H/OL). We then discuss the reliability and limitations of the Chinese
51 dataset of Holocene gridded REVEALS plant-cover, and its current and potential uses.

52 The dataset is available at the National Tibetan Plateau Data Center (TPDC; Li et al., 2022;
53 <https://data.tpdc.ac.cn/en/disallow/d18d2b7e-25fe-49da-b1bd-2be6014162b0/>).

54

55 **Introduction**

56 Vegetation has undergone changes over the globe during the entire Holocene as a result of climate change from
57 the early Holocene and disturbance from anthropogenic activities from the mid Holocene (e.g. ArchaeoGLOBE,
58 2019; Li et al., 2020; Marquer et al., 2017). Pollen- data mapping can provide insights on temporal and spatial
59 vegetation change at broad continental scales (Huntley and Birks, 1983; Huntley and Iii., 1988; Ren and Zhang,
60 1998; Ren and Beug, 2002). However, quantification of past vegetation change based on fossil pollen data is
61 necessary for specific research questions on the relationship between plant cover and e.g. climate or biodiversity.
62 Techniques such as biomization (Prentice and Webb III, 1998) and Modern Analog Technique (MAT) (Overpeck
63 et al., 1985) were widely applied to reconstruct past continental-scale changes in vegetation cover. These
64 techniques have the disadvantage that they cannot quantify the cover of individual plant taxa. In this paper, we
65 present the first pollen-based quantitative reconstruction of Holocene plant-cover change in temperate and northern
66 subtropical China using the Regional Estimates of VEgetation Abundance from Large Sites (REVEALS) model
67 (Sugita, 2007a).

68 The possible effects of anthropogenic land-cover (LC) transformation due to past land-use (LU) change (LULC
69 changes) on Holocene climate is still an issue of debate (Harrison et al., 2020). Current earth system models (ESMs)
70 take care of the climate–land vegetation interactions by coupling a dynamic vegetation model (DVM) with the
71 climate model (e.g. Claussen et al., 2013; Lu et al., 2018; Wyser et al., 2020). DVMs simulate climate-induced
72 (natural) vegetation. Therefore, estimates of past LULC changes have to be estimated to study their effect on past
73 climate. The anthropogenic land-cover change scenarios (ALCCs) most commonly used by palaeoclimate

74 modelers are those from the HYDE database (Klein Goldewijk et al., 2017) and the KK10 dataset of past
75 deforestation (Kaplan et al., 2009). These scenarios are based on a number of assumptions on population growth,
76 per-capita land use, and other parameters influencing land use over time in the past (e.g. Kaplan et al. 2017).
77 Therefore, a current priority is to produce datasets of pollen- and archaeology-based data of past LU and LC that
78 can be used in palaeoclimate modeling or the evaluation of DVMs and ALCCs (PAGES LandCover6k (Gaillard
79 et al., 2015; Morrison et al., 2016; Harrison et al., 2020)).

80 The only gridded pollen-based REVEALS reconstructions of plant cover for the purpose of climate modeling
81 published so far are those for NW-Central Europe North of the Alps (five time windows of the Holocene)
82 (Trondman et al., 2015) and entire Europe through the Holocene (11.7 ka BP to present) (Githumbi et al., 2022).
83 A comparison of Trondman et al. (2015) reconstruction with the ALCC scenarios from HYDE 3.1 (Klein
84 Goldewijk et al., 2011) and KK10 (Kaplan et al., 2009) suggests that the KK10-simulated deforestation is closer
85 to the REVEALS estimates of open land (OL) cover than the HYDE 3.1 deforestation (Kaplan et al., 2017). In a
86 study using a regional climate model (Strandberg et al., 2014), it was found that the effect on mean summer and
87 winter temperatures of anthropogenic deforestation equaling KK10-simulated deforested land in Europe between
88 6 and 0.2 ka BP varied between ca. -1 °C and +1 °C depending on the season and geographical location. This
89 indicates that LULC **changes** in the past did matter in terms of climate change and was further confirmed in a
90 recent palaeoclimate modelling study of the climate at 6 ka BP using the latest pollen-based REVEALS
91 reconstruction of plant cover in Europe (Githumbi et al., 2022; Strandberg et al., 2022). **Given that the gridded
92 REVEALS reconstructions are not continuous over space, i.e. only a part of the grid cells have pollen-based
93 REVEALS estimates of plant cover, such a dataset is comparable to a collection of point data in space. It implies
94 that the REVEALS data need to be interpolated over space to produce a true gridded dataset with values of plant
95 cover in all grid cells. Such interpolations were performed using the European gridded REVEALS reconstructions
96 (e.g. Pirzamanbein et al., 2012; Githumbi et al., 2022; Strandberg et al., 2022) and used for the first time in climate
97 modelling by Strandberg et al. (2022).** Besides the gridded REVEALS reconstructions at the continental scale of
98 Europe mentioned above, gridded REVEALS reconstructions along N-S and W-E transects through Europe
99 between 11.7 ka BP and present were used to disentangle the effects of climate and land-use change on Holocene
100 vegetation (Marquer et al., 2017). Moreover, gridded maps of pollen-based REVEALS estimates of open land
101 cover in the northern hemisphere (N of 40°) were published for a couple of Holocene time windows (Dawson et
102 al., 2018).

103 Several reconstructions of the biomes (Ni et al., 2010, 2014) and vegetation cover (Tian et al., 2016) of China
104 during the Holocene are available. However, these reconstructions do not provide quantitative information on the
105 spatial extent of deforested land within woodland biomes or vegetation types including both trees and herbs.
106 Therefore, they are of limited value for use in palaeoclimate modelling or the evaluation of DVM-simulated
107 vegetation cover or ALCC scenarios.

108 The dataset of gridded pollen-based REVEALS estimates of plant cover for temperate and northern sub-tropical
109 China presented in this paper is based on the REVEALS estimates published in Li et al. (2020). It includes, for 25
110 consecutive time windows of the Holocene, cover estimates for 27 plant taxa, further grouped into estimates of
111 cover for six plant functional types (PFTs) and three land-cover types (LCTs), i.e. coniferous tree (CT),
112 broadleaved tree (BT) and C3 herbs/open land (C3H/OL). PFTs are either single taxa (mainly genus, such as *Pinus*,

113 *Betula*, etc.) or groups of taxa. The REVEALS estimates for the 27 plant taxa are exactly the same as in Li et al.
114 (2020), while grouping of taxa into PFTs and LCTs is different. The latter is explained in the Method section
115 below. Here we briefly describe the methods used and their rationales, present a selection of maps of the cover of
116 CT, BT and C3H/OL for eight time windows of the Holocene, and discuss the reliability and limitations of the
117 dataset as well as its current and potential uses. The entire dataset is available at
118 <https://data.tpdc.ac.cn/en/disallow/d18d2b7e-25fe-49da-b1bd-2be6014162b0/>. The major differences between Li
119 et al. (2020) and this paper are the purpose, visualization of the data, and discussion of the dataset. While Li et al.
120 (2020) visualize the results over time for each reconstruction and focus on Holocene changes in openland versus
121 woodland cover and their interpretation in terms of land-use and/or climate-induced changes, the present paper
122 has the major purpose to make the data available to users, in particular climate and vegetation modellers, and
123 explain its potentials and limitations; moreover, it visualizes the results in space and only for a few selected time
124 essentially to provide an illustration of the dataset that says more to the reader than an excel file with numbers.

125

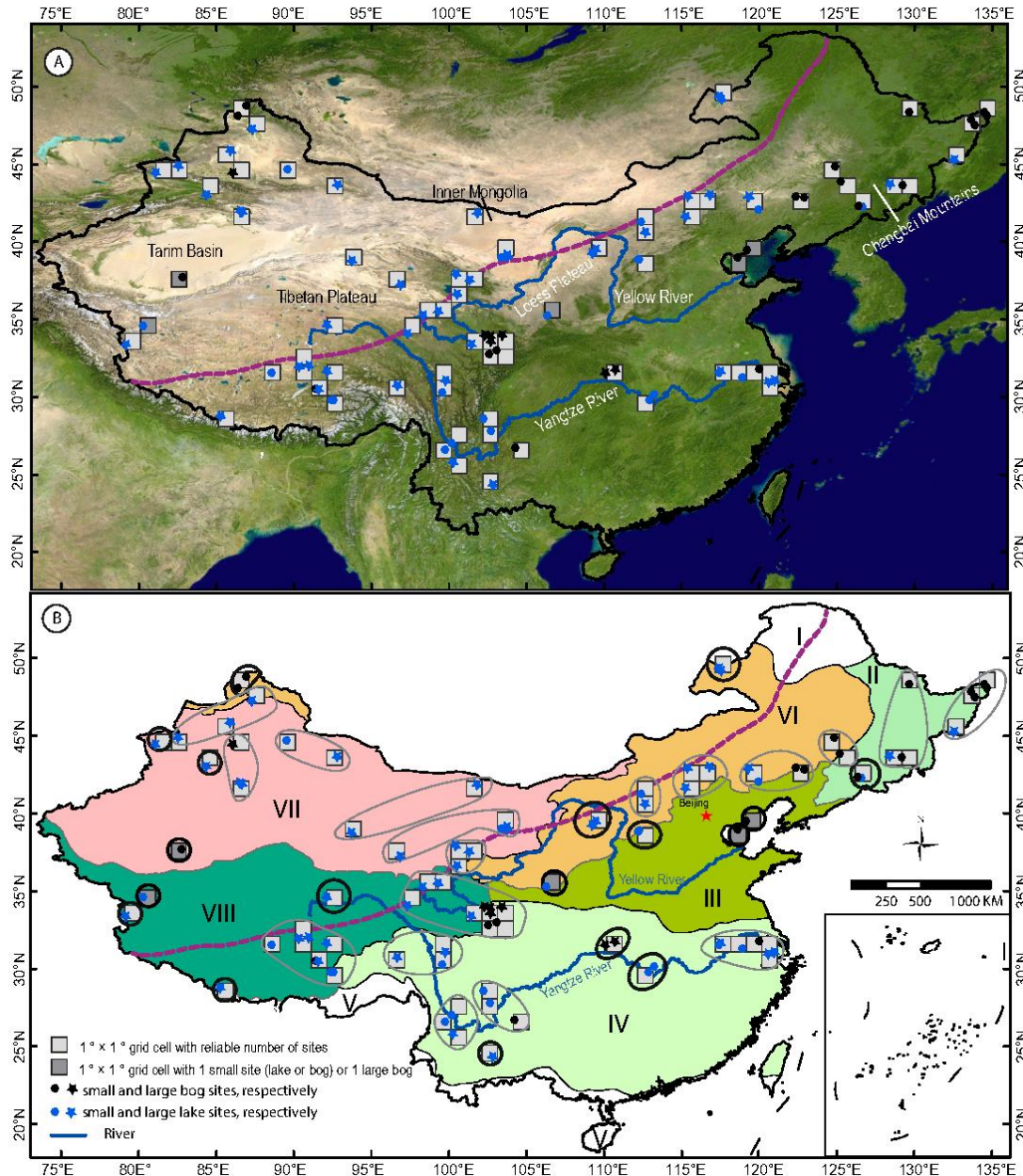
126 **2 Data and methodology**

127 For the sake of consistency and comparison between regions and continents, and to fulfil the criteria required for
128 a contribution to the Past Global Changes (PAGES) LandCover6k working group (2015–2021;
129 <https://pastglobalchanges.org/science/wg/former/landcover6k/intro>), the application of the REVEALS model
130 follows the protocol used for the REVEALS reconstructions performed in Europe (Mazier et al., 2012; Trondman
131 et al., 2015) as closely as possible. For the full protocol of the REVEALS reconstructions for China, see Li et al.
132 (2020).

133 **2.1 Pollen data**

134 The pollen records selected for this study are from the pollen-data archive published by Cao et al. (2013) and from
135 individual contributors. The pollen-data archive includes over 230 pollen records for temperate and northern
136 subtropical China covering all or parts of the Holocene. However, only 94 pollen records met the criteria required
137 for a contribution to PAGES LandCover6k (Trondman et al., 2015; Githumbi et al., 2022): i.e. the pollen records
138 are from lake sediments and/or peat deposits in small to large basins, pollen identification is of good quality, their
139 chronology is based on ≥ 3 dates (^{14}C or other types of dates), and they have a temporal resolution of minimum
140 two pollen counts per 500 years. All chronologies were carefully examined. If required, new age-depth models
141 were established using the BACON software (Blaauw and Christen, 2011). Hereafter, all ages are given in ka BP
142 (1000 years before present; BP= 1950 CE).

143 The metadata table (Table S1) includes, for each pollen record/site, the vegetation zone, the number of the site
144 group (Gr; explanations below), the site name and its latitude, longitude and elevation, the province, the site size
145 (area and calculated radius) and type (lake or bog), the type of pollen data (original raw pollen counts, or calculated
146 pollen counts using information from published pollen diagrams), the dating method and number of dates, the
147 timespan covered by the pollen record, the mean time resolution of the pollen counts, and the literature reference.



148

149 **Figure 1: Study region and selected Holocene pollen records. A. Satellite image from planet observer showing the major**
 150 **mountains, rivers and geographical regions mentioned in the text. B. Map from Li et al. (2020), modified: vegetation**
 151 **zones in China following Hou (2019). The REVEALS reconstructions are either representing plant cover in a single**
 152 **grid cell (emphasized by a thick black line) or several grid cells (diminished by a grey line). Grid cell reliability in terms**
 153 **of REVEALS estimates of plant cover is indicated by fill colours, light grey for high reliability and dark grey for low**
 154 **reliability, as defined on the basis of the number, size, and type of pollen sites (see text for detailed explanations). Roman**
 155 **numbers refer to vegetation zones: I. Boreal forest, II. Coniferous-deciduous mixed forest, III. Temperate deciduous**
 156 **forest, IV. Subtropical broadleaved evergreen and deciduous forest, V. Tropical monsoonal rainforest, VI. Temperate**
 157 **steppe, VII. Temperate desert, VIII. Highland vegetation.**

158

159 2.2 The REVEALS model and rationales for the model-application protocol

160 A full description of the REVEALS model and its assumptions is published in Sugita (2007a). The model was
 161 developed to estimate plant cover at a regional scale using pollen data from large lakes. It is a modification of the
 162 R-Value model (Davis, 1963) that corrects pollen percentage biases caused by inter-taxonomic differences in
 163 pollen productivity and dispersion. Empirical tests in southern Sweden and northern America suggest that pollen

164 records from lakes ≥ 50 ha provide reliable pollen-based REVEALS estimates of regional plant cover (Hellman et
165 al., 2008a,b; Sugita et al., 2010). The rationales behind the general protocol used for the gridded REVEALS
166 reconstructions are presented in detail in Mazier et al. (2012), and Trondman et al. (2015). Major rationales are
167 those motivating the use of a $1^\circ \times 1^\circ$ spatial resolution (grid-cell size), a 500 years time resolution (except for the
168 three most recent time windows), and all suitable pollen records from large and small sites. The choice of the
169 spatial scale is based on a test performed in southern Sweden demonstrating that REVEALS estimates of modern
170 plant cover using pollen assemblages from surface lake sediments were in good agreement with the actual plant
171 cover within areas of $50 \text{ km} \times 50 \text{ km}$ and $100 \text{ km} \times 100 \text{ km}$ (Hellman et al., 2008b). In addition, this spatial scale
172 is appropriate for palaeoclimate modelling, either with global or regional climate models (e.g. Strandberg et al.,
173 2014; 2022). The time resolution is motivated by the influence of the size of pollen counts on the size of the
174 REVEALS estimates standard errors. A time resolution of 500 years ensures that a maximum of the REVEALS
175 reconstructions have low SEs and it is still meaningful for the study of past land-cover changes over several
176 millennia. As pollen counts are generally available at a higher time resolution for the last 1000 years, and because
177 land-cover changes were often more rapid during the recent millennium than through the earlier millennia, the
178 length of the three most recent time windows were fixed to 350 (0.7–0.35 ka BP), 250 (0.35–0.1 ka BP), and 100
179 + x years (0.1 ka BP to present (1950 CE + x years, where x years is the number of years between 1950 CE and
180 the year of coring)). The relevance and suitability of using pollen records from both large and small sites for
181 REVEALS applications in order to increase the reliability of the pollen-based estimates of plant cover within each
182 grid cell is confirmed by simulation tests in Sugita (2007a) and empirical tests in southern Sweden (Trondman et
183 al., 2016) (see Li et al. (2020) for more details). In the absence of pollen records from large lakes, the larger the
184 number of small sites (lakes or bogs), the better the REVEALS result. However, bogs (large and small) violate
185 one of the assumptions of the REVEALS model, i.e. “no vegetation is growing on the deposition basin” (Sugita,
186 2007a). Violation of this assumption has been shown to bias REVEALS results most significantly in the case of
187 large bogs, while pollen records from multiple small bogs use to provide reliable estimates of plant cover (Mazier
188 et al., 2012; Trondman et al., 2016).

189 In this gridded REVEALS reconstruction of plant cover in China, a deviation from the standard protocol used in
190 Europe has been to perform the REVEALS reconstructions using pollen records within larger areas than a single
191 $1^\circ \times 1^\circ$ grid cell. Due to the low spatial density of the 94 selected pollen records in this study, the pollen records
192 were grouped for the application of the REVEALS model within coherent regions with comparable
193 biogeographical characteristics and similar vegetation histories (see Li et al. (2020) for details). It implies that, in
194 these cases, the grid cells covered by a group of pollen sites (varies between 2 and 8 grid cells, Fig. 1) have
195 the same REVEALS estimates, i.e. the same mean vegetation cover (Figures 2-4). The advantage is that the
196 REVEALS estimates are more reliable and have lower SEs than REVEALS estimates obtained for individual
197 $1^\circ \times 1^\circ$ grid cells with only one or two pollen records. The pollen records within 57 of 75 $1^\circ \times 1^\circ$ grid cells belong to
198 such groups of pollen records (19 in total) covering several grid cells. The remaining 18 grid cells include one or
199 two pollen records only and are emphasized in Figure 1. In these cases, no additional pollen record(s) were
200 available in nearby grid cells, and the REVEALS application was performed with these few pollen records for
201 each grid cell separately. Several of these reconstructions are based on a single large bog or 1-2 small sites and
202 should therefore be considered as less reliable.

203

204 2.3 Parameter settings, REVEALS runs and calculation of cover for groups of plant taxa

205 Parameters needed to run the REVEALS model are relative pollen productivity estimates (RPPs) and their standard
206 deviation (SD), fall speed of pollen (FSP), maximum extent of regional vegetation (Z_{\max} ; km), wind speed (m/s),
207 and atmospheric conditions (expressed by four parameters, i.e. vertical and horizontal diffusion coefficients, a
208 dimensionless turbulence parameter, and wind speed (see Jackson and Lyford, 1999 for details)). We used the
209 mean RPPs estimates with their related SDs and the FSPs of 27 plant taxa from the synthesis of available RPP and
210 FSP values in temperate China (Li et al., 2018b), a Z_{\max} of 100 km, a wind speed of 3 m/s, and neutral atmospheric
211 conditions. Note that, in contrast to Cao et al. (2020), Li et al. (2020) chose to use only RPP estimates obtained
212 from pollen-vegetation datasets collected in temperate China. It implies that two important taxa in northwestern
213 China are missing from the reconstruction, namely *Abies* and *Picea*. Cao et al. (2020) used the RPP estimates of
214 *Abies* and *Picea* from Europe assuming that differences in species between Europe and China would not influence
215 significantly their RPP. As long as this assumption is not tested we decided to keep the principle used in Li et al.
216 (2020) for the dataset we are publishing here. The 27 taxa included in this REVEALS reconstruction account
217 for >50% of the total pollen from all pollen taxa in all records, and for > 80% of the total pollen from all pollen
218 taxa in most records.

219 Other parameters needed are the basin type (lake or bog) and its size (radius in m). We applied two models of
220 pollen dispersion and deposition, the “Prentice model” (Prentice, 1985) for bogs and the “Prentice-Sugita” model
221 (Sugita, 1993) for lakes.

222 Before running the REVEALS model, the pollen counts of the 27 plant taxa within each time window were
223 summed up in each pollen record. The REVEALS model was run separately with pollen records from bogs (with
224 the Prentice’s model) and lakes (with the Prentice-Sugita model) for each group of pollen records. These model
225 runs result in two different mean REVEALS estimates (and their standard errors, SEs) of cover for the 27 plant
226 taxa, one from bog(s) and one from lake(s). The standard deviations (SD) of the RPPs are taken into account in
227 the calculation of the REVEALS standard errors (SEs), as well as the number of pollen grains counted in the
228 sample (Sugita, 2007a). The final mean REVEALS estimates of cover for the 27 plants taxa (from bog(s) + lake(s))
229 are then calculated. The SEs of the final mean REVEALS estimates for each group of pollen records are obtained
230 using the delta method (Stuart and Ord, 1994) and derived from the sum of the within- and between-site variations
231 in the REVEALS results in the grid cell (see Li et al., 2020 for details). The latest version of the REVEALS
232 computer program, LRA.REVEALS.v6.2.4.exe (Sugita, unpublished) and example files are available at the link
233 <https://1drv.ms/u/s!AkY-0mVRwOaykdgmINfXVSc-4t4n5w?e=7U55hO>. It implements all calculations
234 mentioned above.

235 For use in climate models and evaluation of HYDE, KK10, and DVMs (see Introduction), we also calculated the
236 mean REVEALS estimates (and their SEs) of cover for groups of taxa, i.e. plant functional types (PFTs) and land-
237 cover types (LCTs). To do so, the 27 plant were harmonized with six PFTs defined for China by Ni et al. (2010,
238 2004), and with the three LCTs CT, BT and C3H/OL (Table 1). Note that Li et al. (2020) used slightly different
239 PFTs where Cupressaceae, Poaceae, Cyperaceae and Rosaceae were treated as separate PFTs to make the
240 interpretation of changes in the amount of conifers and herbs in terms of regional versus local - and natural versus
241 anthropogenic - vegetation easier. Moreover, Rubiaceae and Elaeagnaceae were classified as belonging to the
242 temperate shade-tolerant broadleaved evergreen trees, and *Castanea* and *Juglans* were grouped with the herbs

243 (openland) and anthropogenic indicators (including planted trees). In this paper we used the PFT classification
 244 provided in Table 1 in which Cupressaceae is grouped with *Pinus* as belonging to PFT TeNE (temperate shade-
 245 intolerant needle-leaved evergreen trees), Elaeagnaceae, *Castanea*, *Juglans* with broadleaved trees as belonging
 246 to PFT TeBS (Temperate shade-tolerant broadleaved summer green trees), and Cyperaceae, Poaceae, Rosaceae,
 247 and Rubiaceae with all herbs as belonging to PFT C3H/OL (C3 Herbs/openland). We propose that this
 248 classification is more appropriate for use in climate modelling contexts than that used in Li et al. (2020) in which
 249 the major aim of the study was to interpret the pollen-based plant-cover reconstruction in terms of open land versus
 250 woodland cover.

251 For more details on parameter setting, REVEALS runs, models of pollen dispersion and deposition, and the delta
 252 method, the reader is referred to Li et al. (2020).

253 Table 1: Aggregation of pollen morphological types into Land-cover types (LCTs) and plant functional types (PFTs) (following
 254 Ni et al., 2010, 2014). Fall speed of pollen (FSP) and mean relative pollen productivities (RPPs) with standard deviation (SD)
 255 in brackets (dataset Alt2 of Li et al., 2018b). The number of values available in the calculation of the mean RPPs and location
 256 of the RPP studies in terms of vegetation zones are also provided. Roman numbers refer to the vegetation zones: I. Boreal
 257 forest, II. Coniferous-deciduous mixed forest, III. Temperate deciduous forest, IV. Subtropical broadleaved evergreen and
 258 deciduous forest, V. Tropical monsoonal rainforest, VI. Temperate steppe, VII. Temperate desert, VIII. Highland vegetation.

Land cover types	PFTs	PFTs definition	Plant taxa/Pollen-morphological types	FSP(m/s)	RPP(SD)	Number of RPPs	Location of RPP studies (Vegetation zones)
Coniferous Tree	TeNE	Temperate shade-intolerant needle-leaved evergreen trees	<i>Pinus</i>	0.035	18.37(0.48)	4	II, III,
			Cupressaceae	0.010	1.11(0.09)	1	III
	BNS	Boreal needle-leaved summer green trees	<i>Larix</i>	0.126	2.14(0.24)	3	II, III
Broadleaved Trees	IBS	Boreal shade-intolerant broadleaved summer green trees	<i>Betula</i>	0.014	12.42(0.12)	3	II, III
			<i>Castanea</i>	0.004	11.49(0.49)	1	III
	TeBS	Temperate shade-tolerant broadleaved summer green trees	Elaeagnaceae	0.012	8.88(1.30)	1	III
			<i>Fraxinus</i>	0.017	3.94(0.73)	1	II
			<i>Juglans</i>	0.031	7.69(0.24)	1	III
			<i>Quercus</i>	0.019	5.19(0.07)	3	II, III
			<i>Tilia</i>	0.028	0.65(0.11)	1	II
			<i>Ulmus</i>	0.021	4.13(0.92)	2	II,III
	TeBE	Temperate shade-tolerant broadleaved evergreen trees	<i>Castanopsis</i>	0.004	11.49(0.49)	1	III
			<i>Cyclobalanopsis</i>	0.019	5.19(0.07)	3	II,III
Openland	C3H	C3 Herbs	Amaranth./Chenop.	0.013	4.46(0.68)	2	VI, VIII
			<i>Artemisia</i>	0.010	21.15(0.56)	4	II, VI
			Asteraceae	0.019	4.4(0.29)	2	VI
			Brassicaceae	0.012	0.89(0.18)	1	III
			<i>Cannabis/Humulus</i>	0.010	16.43(1.00)	1	III
			Convolvulaceae	0.043	0.18(0.03)	1	VI
			Cyperaceae	0.022	0.44(0.04)	2	III, VIII
			Fabaceae	0.017	0.49(0.05)	2	III, VI,
			Lamiaceae	0.015	1.24(0.19)	2	VI
			Liliaceae	0.013	1.49(0.11)	1	VI
			Poaceae	0.021	1(0)	6	II, III, V, VI, VIII
			Ranunculaceae	0.007	7.77(1.56)	1	II
			Rosaceae	0.009	0.22(0.09)	1	VI
Rubiaceae	0.010	1.23(0.36)	1	III			

259

260 **2.4 Data format**

261 The dataset of pollen-based REVEALS estimates of Holocene plant cover for temperate and northern sub-tropical
262 China comprises four csv files with the REVEALS proportions of plant cover (and related SEs) in 75 1°x 1° grid
263 cells and 25 time windows for 27 taxa (Data1.plants.csv), six PFTs (Data2.6PFTs.csv) (PFT classification as in
264 Table 1), three land-cover types (Data3.LCTs.csv) and ten PFTs (Data4.10PFTs.csv) (PFT classification as in Li
265 et al. (2020)). Two additional files are complementing the REVEALS dataset, the metadata file (Table S1) (see
266 section 2.1 pollen data for details) and a table providing details on the number and types of sites used in the
267 REVEALS reconstruction for each grid cell and each time window (Table S2). The REVEALS excel data files
268 and Tables S1 and S2 (also in Supplementary Material) are available at
269 <https://data.tpd.ac.cn/en/disallow/d18d2b7e-25fe-49da-b1bd-2be6014162b0/>.

270

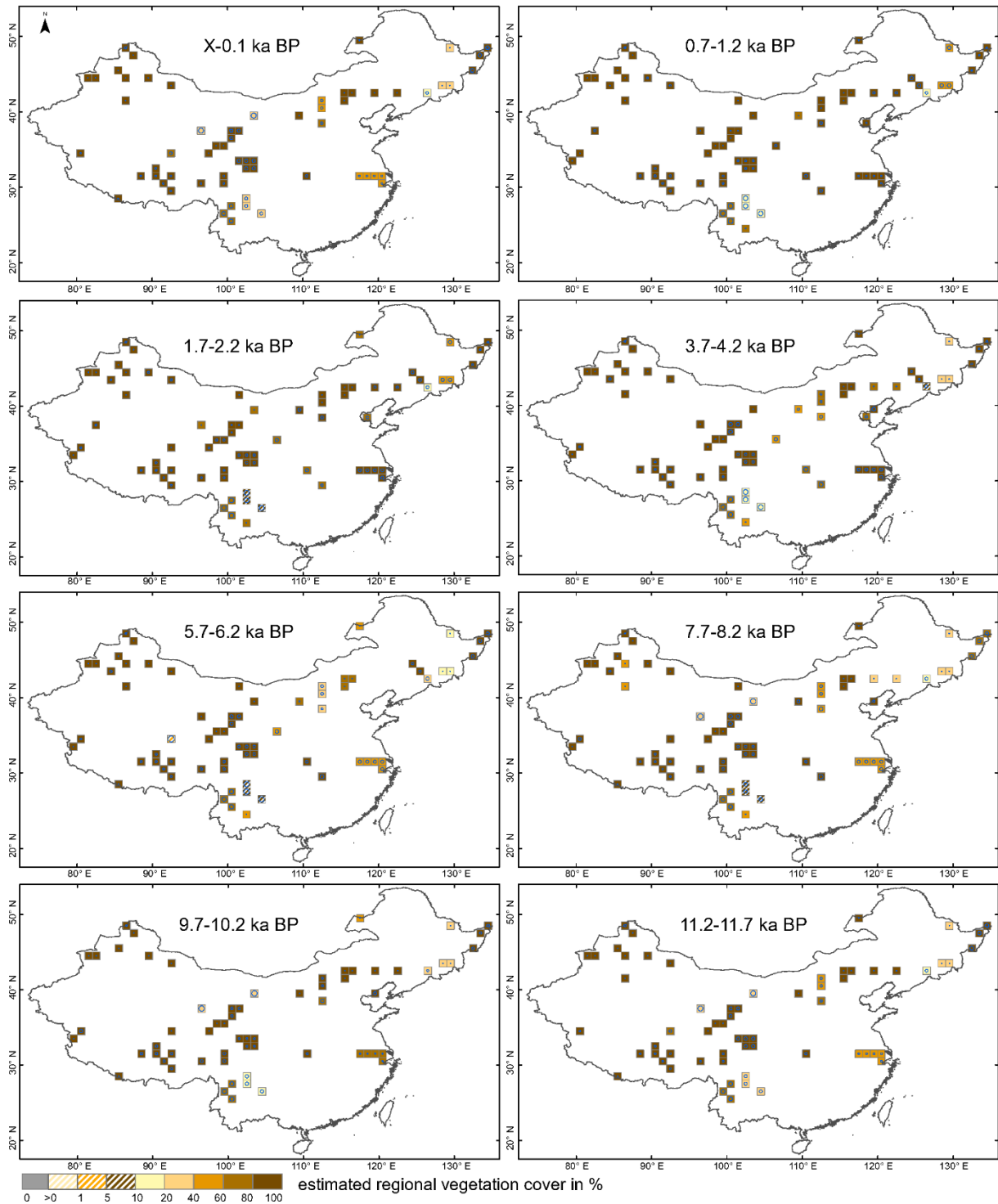
271 **3. Results**

272 As an illustration, we describe below maps of the REVEALS reconstructed cover for the three land-cover types
273 CT, BT and C3H/OL for eight selected time windows of the Holocene that provide snap shots in time of
274 significantly different composition of land-cover types between 11.7 ka BP and present. For each land-cover type
275 the maps are described from the oldest (11.7–11.2 ka BP) to the youngest (0.1 ka–present) map, and the map for
276 each time window is described in comparison to the map for the earlier time window (e.g. for the 9.7–10.2 ka BP
277 map, changes are expressed in comparison to the 11.7–11.2 ka BP map). Land-cover changes (decrease or increase)
278 are expressed in absolute fractions, e.g. an increase of 20% at 9.7–10.2 ka BP from a cover of 50% of the grid cell
279 at 11.7–11.2 ka BP implies that the cover at 9.7–10.2 BP is 70% of the grid cell. The descriptions start with
280 information extracted from Li et al. (2020) on the modern occurrence and Holocene history (in terms of pollen-
281 based REVEALS cover) of the taxa constituent of the land-cover type in question.

282 **3.1 Open Land (C3H/OL; Figure 2)**

283 OL is the sum of the reconstructed cover of 14 herb taxa for which RPPs are available. Poaceae, Cyperaceae,
284 Amaranthaceae/Chenopodiaceae and *Artemisia* are often represented by high pollen percentages during the
285 Holocene. Other herbs that can be relatively well represented during most of the Holocene are Asteraceae,
286 Brassicaceae, Ranunculaceae, Rosaceae, and Rubiaceae. Pollen from Convolvulaceae, Fabaceae, Lamiaceae and
287 Liliaceae can be quite common over some periods of the Holocene, while *Cannabis/Humulus* is not frequent.
288 These herbs characterize today primarily open vegetation, i.e. temperate xerophytic shrubland and grassland, desert,
289 and tundra, as well as human-induced vegetation (cultivated and grazing land). The REVEALS reconstructions
290 suggest that the cover of Poaceae, Cyperaceae and Rosaceae during the Holocene is often equal or larger than the
291 cover of all remaining 11 herbs together, although *Artemisia* and Amaranthaceae/Chenopodiaceae can also reach
292 a relatively large cover (Li et al., 2020).

293 The time window 11.7–11.2 ka BP is characterized by OL cover values >80% in most of northwestern China and
294 the Tibetan Plateau. OL values of 40–60% or 60–80% are found in parts of southwestern China and Inner
295 Mongolia. OL values of 40–60% occur also in the lower reach of the Yangtze River region, and values of 20–40%
296 or 10–20% in northeastern China. The time window 10.2–9.7 ka BP shows an increase in OL cover of 10% in
297 northeastern China, and an increase to 60–80% or > 80% in part of Inner Mongolia and the lower reach of the



298

299 **Figure 2. Grid-based REVEALS estimates of C3 herbs/Open Land (C3H/OL) cover for eight selected time windows of**
 300 **the Holocene. Percentage cover in intervals of 1% (>0–1%), 4% (>1–5%), 5% (>5–10%), 10% (>10–20%), and 20%**
 301 **(>20–100%) represented by increasingly darker colours from >0–1% to >5–10% and from >10–20% to 80–100%.**
 302 **Grid cells without pollen data for the time window, but with pollen data in other time windows are shown in grey.**
 303 **Uncertainties on the REVEALS estimates are illustrated by blue circles of various sizes corresponding to the coefficient**
 304 **of variation (standard error (SE) divided by the grid cell mean REVEALS estimate (RE)). If $SE \geq RE$, the blue circle**
 305 **fills the entire grid cell. $SE \geq RE$ also implies that RE is not different from zero, which is the case primarily for low RE**
 306 **values.**

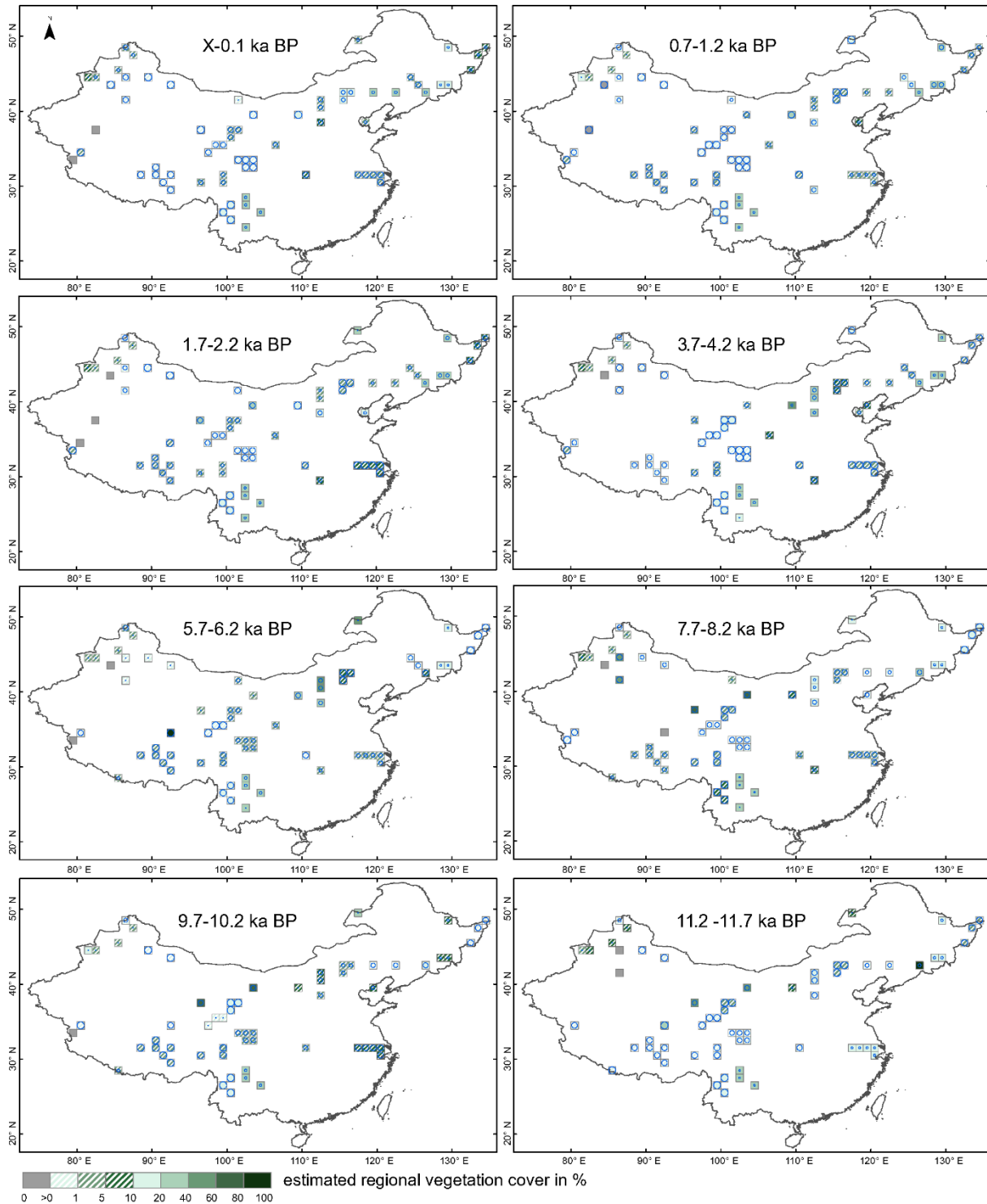
307

308 Yangtze River basin, while a decrease of 20% is seen in part of southwestern China. At 8.2–7.7 ka BP, the OL
309 cover declines in most of the reconstructions, most drastically in parts of the Loess Plateau, central Inner Mongolia
310 and the lower reach of the Yangtze River region, where OL decreased with 20–40%, whilst a decrease of 10–20%
311 is seen in parts of northwestern China. At 6.2–5.7 ka BP, OL shows a further decrease of 20% in Inner Mongolia,
312 northeastern China, and southwestern China, and a decrease of 60% on the central Tibetan Plateau. In contrast, an
313 increase of 40% is observed in part of northwestern China. At 4.2–3.7 ka BP, OL cover is > 80% in most of the
314 regions of northwestern China. An increase of 50% is observed in the lower reach of the Yangtze River region and
315 Inner Mongolia, 20% in part of the Loess Plateau and southwestern China, and 10–20% in part of northeastern
316 China. In contrast, a decrease of OL cover of 10–30% is seen in part of northeastern China. At 2.2–1.7 ka BP, OL
317 cover has increased in almost all regions except for a decrease of 20% in southwestern China. The increase of OL
318 cover is of 40% in Inner Mongolia and Shanxi, and 20% in part of the Changbai Mountain region. Over the last ca.
319 100 years (0.1 ka BP–present), there is no major change in OL cover, except an increase of 10% in southwestern
320 China and a decrease of 20% in part of northeastern China.

321 3.2 Coniferous Trees (CT; Figure 3)

322 CT is the sum of the reconstructed cover of three conifer taxa for which RPPs are available, *Pinus* and
323 Cupressaceae (PFT TeNe) and *Larix* (PFT BNS) (Table 1). We chose to use only RPP values estimated in China
324 (RPP synthesis of Li et al. (2018b)) and, therefore, did not produce REVEALS estimates of the cover of *Abies* and
325 *Picea* (Li et al., 2020). Today, these two taxa are common together with *Pinus* and *Larix* in the boreal forests and
326 coniferous-broadleaved mixed woodlands (zones I and II, respectively). *Abies* and *Picea* also form woodland
327 patches in the westernmost part of the subtropical broadleaved evergreen and deciduous forest (zone IV), and
328 *Abies* and *Pinus* characterize the woodlands of the zone IV southwestern part. Of the three conifer taxa for which
329 REVEALS reconstructions are available, *Pinus* is the one with significant cover over most of the Holocene in all
330 regions characterized by coniferous woodland (or woodland patches) today in central and eastern-northeastern
331 China (Li et al., 2020). *Pinus* has a relatively large cover throughout the Holocene in zone IV southwestern part,
332 zone VI western part and zone II central part, while it has lower cover in zone IV eastern part. Some cover of *Pinus*
333 has some cover from 7 ka BP in zone VI eastern part and relatively high cover from 4.5 ka BP in zone II
334 southeastern part and zone III eastern part. A significant cover of Cupressaceae was reconstructed for the early
335 Holocene from some pollen records in zone IV western part and zone VII easternmost part (temperate desert), and
336 for most of the Holocene in zone VI western and northernmost parts (temperate steppe) (Li et al. 2020). *Larix* is
337 represented in zones II and VI central and northernmost parts either by continuous high cover throughout the
338 Holocene alternatively the Late Holocene only, or by scattered occurrences of high cover through time (Li et al.,
339 2020).

340 There is a consistent increase in CT cover in most grid cells over northern China during the first half of the
341 Holocene with maximum values sometime between 8 and 5 ka BP (the timing depending of the region), before a
342 steady decline of the values of CT cover. The time window 11.7–11.2 ka BP is characterized by CT cover values
343 of over 80% in part of northeastern China, 10–20% or 20–40% in southwestern China, and 10–20% in the eastern
344 part of northwestern China and in the lower reach of the Yangtze River region. Elsewhere CT cover is lower than
345 10%. At 10.2–9.7 ka BP, the CT cover values have decreased in almost all regions, with a decline of 10%



346

347 **Figure 3. Grid-based REVEALS estimates of Coniferous Trees (CT) cover for eight selected time windows of the**
 348 **Holocene. Percentage cover in intervals of 1% (>0–1%), 4% (>1–5%), 5% (>5–10%), 10% (>10–20%), and 20%**
 349 **(>20–100%) represented by increasingly darker colours from >0–1% to >5–10% and from >10–20% to 80–100%.**
 350 **Grid cells without pollen data for the time window, but with pollen data in other time windows are shown in grey.**
 351 **Uncertainties in the REVEALS estimates are illustrated by blue circles of various sizes corresponding to the coefficient**
 352 **of variation (standard error (SE) divided by the grid cell mean REVEALS estimate (RE)). If $SE \geq RE$, the blue circle**
 353 **fills the entire grid cell. $SE \geq RE$ also implies that RE is not different from zero, which is the case primarily for low RE**
 354 **values.**

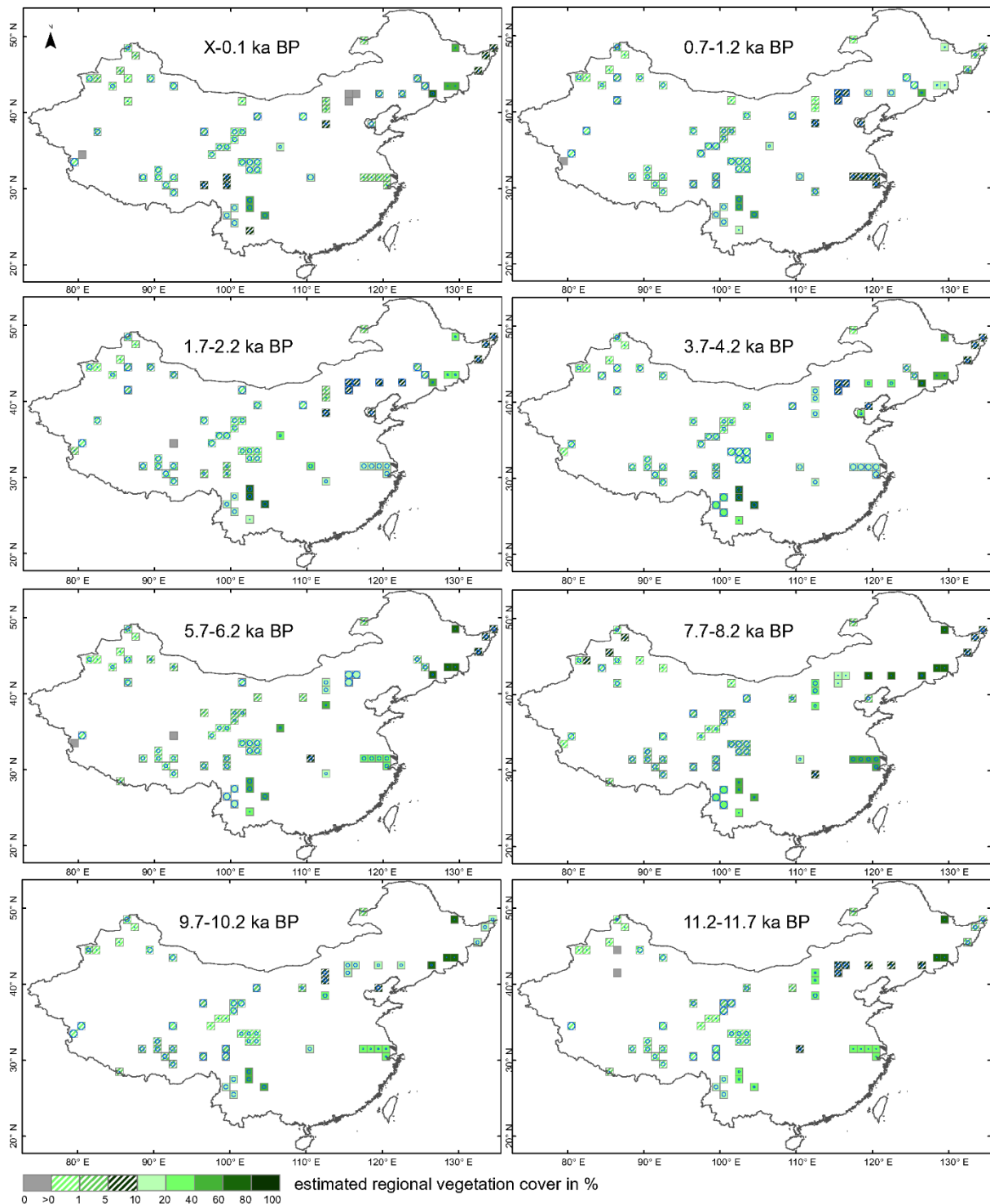
355

356 in the lower reach of the Yangtze river, and 10–20% or 20–40% in part of northwestern China. CT cover is slightly
357 higher in the 8.2–7.7 ka BP time window in most of northeastern China (10–20%), while a small drop is seen in
358 the western part of southwestern China and eastern part of northwestern China. The time window 6.2–5.7 ka BP
359 is characterized by a decrease of CT cover with 10–20% in northeastern China and 40% or 60% in part of
360 northwestern China. In contrast, CT cover has increased with 20–40% and ca 5% in Inner Mongolia and
361 southwestern China, respectively. From 4.2–3.7 ka BP, CT cover exhibits a further decrease with maximum 20%
362 in most of Inner Mongolia and southwestern China. The CT cover at 2.2–1.7 ka BP is even lower, with a decline
363 of 10% and >10–20% in the eastern part of northwestern China and the western part of northeastern China,
364 respectively. There is however a slight increase in CT cover with 2% in northwestern China and the lower reach
365 of the Yangtze River. At 1.2–0.7 ka BP, the CT cover has decreased with 2% on the Tibetan Plateau, in
366 northwestern China, and the lower reach of the Yangtze River. An increase in CT cover with ca. 10% during the
367 last century (0.1 ka BP–present) is found in southwestern, eastern, and most of northeastern China, while a
368 decrease is seen in some parts of northeastern China.

369 3.3 Broadleaved Trees (BT; Figure 4)

370 BT is the sum of the reconstructed cover of ten broadleaved tree taxa for which RPPs are available, *Betula* (PFT
371 IBS), *Castanea*, *Eleagnaceae*, *Fraxinus*, *Juglans*, *Quercus*, *Tilia*, and *Ulmus* (PFT TeBS), *Castanopsis* and
372 *Cyclobalanopsis* (PFT TeBE) (Table 1). *Betula* has a significant cover throughout the Holocene in zone II and
373 most of zone IV (Li et al. 2020). The summer-green broadleaved tree taxa (TeBS) are characteristic of zones II,
374 III and IV with relatively large cover throughout the Holocene, and of the southern boarder of vegetation zone VI
375 with large cover in particular through Mid Holocene. The evergreen broadleaved tree taxa *Castanopsis* and
376 *Cyclobalanopsis* are characteristic of vegetation zone IV with relatively large cover in most of the zone (Li et al.,
377 2020).

378 The Holocene changes in cover of BT show similar trends as those for CT, with a steady increase during the first
379 half of the Holocene with the highest values found in the time windows from 8.2–7.7 ka BP to 5.2–4.7 ka BP
380 (depending on the region) followed by a steady decrease through the Late Holocene. The oldest time window
381 11.7–11.2 ka BP is characterized by the largest BT cover of the Holocene (>80%) in northeastern China, and the
382 second largest BT cover (20–40%) in parts of Inner Mongolia and the lower reach of the Yangtze River region.
383 In contrast, BT cover is <2% in northwestern China and on the Tibetan Plateau. At 10.2–9.7 ka BP, BT cover has
384 increased with ca. 10% in part of northeastern China, while it has decreased with 10% in part of Inner Mongolia.
385 An increase of BT cover with 10% or 20% in time window 8.2–7.7 ka BP is seen in part of northeastern China
386 and the Yangtze River lower reach, while there is a decrease with 5% in northeastern China. At 6.2–5.7 ka BP,
387 BT cover has decreased with 20% in parts of central Inner Mongolia and southwestern



388

389 **Figure 4. Grid-based REVEALS estimates of Broadleaved Trees (BT) cover for eight selected time windows of the**
 390 **Holocene. Percentage cover in intervals of 1% (>0–1%), 4% (>1–5%), 5% (>5–10%), 10% (>10–20%), and 20%**
 391 **(>20–100%) represented by increasingly darker colours from >0–1% to >5–10% and from >10–20% to 80–100%.**
 392 **Grid cells without pollen data for the time window, but with pollen data in other time windows are shown in grey.**
 393 **Uncertainties on the REVEALS estimates are illustrated by blue circles of various sizes corresponding to the coefficient**
 394 **of variation (standard error (SE) divided by the grid cell mean REVEALS estimate (RE)). If $SE \geq RE$, the blue circle**
 395 **fills the entire grid cell. $SE \geq RE$ also implies that RE is not different from zero, which is the case primarily for low RE**
 396 **values.**

397

398 China. A further decrease of cover has occurred 4.2–3.7 ka BP, with 20–30% in the lower reach of the Yangtze
 399 river and northeastern China, and with 10% in Inner Mongolia. BT cover has further decreased at 2.2–1.7 ka BP

400 with 10% in the western and central part of northeastern China, and at 1.2–0.7 ka BP with < 10%, 10%, or 20% in
401 northeastern China and the the Yangtze River lower reach. In the last century (0.1 ka BP–present), BT cover has
402 increased with 30% and 20% in the eastern part of northeastern China and in southwestern China, respectively. In
403 contrast, the western part of northeastern China is characterized by a strong decrease in BT cover.

404 **4. Reliability and limitations of the dataset**

405 **4.1 Accuracy and reliability of the REVEALS estimates of plant cover**

406 For a detailed description of the accuracy and reliability of the REVEALS reconstructions, the reader is referred
407 to Li et al. (2020). The quality of the REVEALS reconstructions are mainly reliant on input data (pollen counts
408 quality and size), the reliability of pollen records chronologies and relative pollen productivities used (RPPs), the
409 type and size of the pollen records sites (lakes or bogs), the number of pollen records used for reconstruction in
410 each grid cell, and variation between pollen counts within a grid cell. The standard errors (SEs) of the REVEALS
411 estimates are a measure of their accuracy and reliability. If $SE < \text{mean REVEALS estimate of cover}$, the result is
412 considered to be reliable, which is the case for over 85% of the reconstructions. If $SE \geq \text{mean REVEALS estimates}$
413 of cover, the result is not different from zero and, therefore, not reliable. The latter occurs mainly in the lower
414 reach of the Yangtze River region.

415 Other issues may influence the reliability of the REVEALS estimates of plant cover. REVEALS was intended for
416 pollen records in large lakes (Sugita, 2007a). Pollen records from bogs violate the assumption of the model that
417 no plants are growing on the surface of the deposition basin. Therefore, pollen-based REVEALS estimates from
418 bogs may be biased by local cover of major plant taxa such as Poaceae and Cyperaceae, in particular if bogs are
419 large. The problem is discussed in detail in Li et al. (2020), where the cover of openland was considered to be
420 overestimated in some grid cells due to this phenomenon, in particular in northeastern China. This issue and the
421 theoretically inadequate application of REVEALS using a single pollen record from a small site (lake or bog) or a
422 large bog in a grid cell are indicated as providing less reliable or unreliable REVEALS reconstructions of plant
423 cover in Figure 1 (dark grey grid cells). Moreover, the number of sites and their type (lake or bog) and size (large
424 or small) are provided for each site group (grid cell) and time window in Table S2. Uncertainty related to the RPPs
425 used is another factor influencing reliability of the REVEALS reconstructions. We use the mean RPPs from the
426 Chinese synthesis published in Li et al (2018b). The assumptions are that RPPs are constant through time and the
427 mean RPPs are a good approximation for the plant taxa over the entire study region. Although we do not know
428 whether RPP was constant through the Holocene for the plant taxa used in the reconstructions, the assumption is
429 necessary if we are to reconstruct changes in the abundance or absolute cover of plants from changes in pollen
430 percentages over time (e.g. Birks and Birks, 1980; Sugita, 2007a). Mean RPPs are most reliable for large regions
431 if they are based on a large number of RPP values that are well distributed within the study region, and if these
432 values do not differ very significantly from each other. A measure of variability among RPP values is provided by
433 the SD of the mean RPP, which is in turn imbedded in the REVEALS estimate's SE of a plant taxon's cover.
434 However, none of the SDs is very large in relation to the mean RPP values we are using (Table 1). SD is larger
435 than a tenth of the mean RPP value for ten taxa of the 27 taxa used (i.e. Elaeagnaceae, *Fraxinus*, *Tilia*, *Ulmus*,
436 *Amaranthaceae/Chenopodiaceae*, *Brassicaceae*, *Convolvulaceae* and *Ranunculaceae*; Table 1), however with SD
437 less than a fifth of the mean RPP value except for *Fraxinus*, *Ulmus*, *Brassicaceae*, and *Ranunculaceae* (SD ca. a
438 fifth of mean RPP), *Rosaceae* (SD ca. a third of mean RPP) and *Rubiaceae* (SD ca. a fourth of mean RPP). There

439 is no way to measure the uncertainty that may be caused by the use of a mean RPP value based on too few RPP
440 values, or RPP values that are not representative of all major vegetation zones of the study region. The number of
441 values available in the calculation of the mean RPPs and location of the RPP studies in terms of vegetation zones
442 are provided in Table 1. This information can be a mean to identify RPPs that might be uncertain for REVEALS
443 land-cover reconstructions in general, or in particular for certain regions. At the time of the analysis, there was
444 only one RPP value for 14 of the 27 taxa in this study, i.e. Cupressaceae, *Castanea*, Elaeagnaceae, *Fraxinus*,
445 *Juglans*, *Tilia*, *Castanopsis*, Brassicaceae, *Cannabis/Humulus*, Convolvulaceae, Liliaceae, Ranunculaceae,
446 Rosaceae, and Rubiaceae. The REVEALS estimates for these taxa should, therefore, be considered with caution.
447 The REVEALS estimates for *Castanopsis* and *Cyclobalanopsis* are also uncertain because, in the absence of RPPs
448 for these two taxa, we used instead the RPPs of *Castanea* and *Quercus*, respectively, assuming comparable pollen
449 productivities between these taxa (see Li et al., 2020 for further details on this issue).

450

451 **4.2 Limitations of the pollen-based REVEALS plant cover**

452 The REVEALS model estimates the proportion of each plant taxon in relation to the total cover of all taxa with
453 RPPs available (in this case 27 taxa) rather than its actual cover if all existing taxa could be considered. The same
454 consideration is valid for the REVEALS cover of the three major land-cover types C3H/OL, CT and BT. This is a
455 serious caveat if the pollen taxa for which no RPP values are available represent a significant part of the pollen
456 assemblages. In this first dataset of REVEALS land-cover estimates, our decision to use exclusively Chinese RPPs
457 and, therefore, not reconstruct the cover of *Abies* and *Picea* is a major issue. This may bias the results in
458 overestimating the cover of C3H/OL in particular, but also of BT. The latter needs to be kept in mind in the
459 interpretation and use of the dataset for regions where *Abies* and *Picea* were common during part of, or the entire
460 Holocene, which was the case mainly in vegetation zones II and IV (see Results for CT for more details).

461 Another important caveat of all REVEALS reconstructions is that the cover of bareground in a landscape cannot
462 be inferred by the model. However, bareground was (and still is) a significant portion of the land cover in regions
463 characterized by desert, steppe, and high altitude vegetation (zones VI, VII and VIII in this study). So far, there is
464 only one attempt at estimating bareground in the past (Sun et al., 2022). It uses the modern relationship between
465 tree pollen and the cover of bareground in northern-central China, and the Modern Analog Technique (MAT) to
466 estimate the past cover of bareground using fossil pollen records from the same region. The MAT-estimated cover
467 of bareground is then used to correct REVEALS-estimated plant cover from the same fossil pollen records. The
468 results suggest that bareground covered 40 to 60% of the land and that the uncorrected REVEALS reconstructions
469 overestimate the cover of trees by ca. 50%, which can have implications if pollen-based REVEALS land cover is
470 used in palaeoclimate model experiments. In the context of palaeoclimate modelling, the interpretation of the
471 openland fraction (with or without bareground) in terms of deforestation (human-induced decrease in tree cover)
472 remains problematic due to the possible occurrence of herb taxa in both natural, climate-induced and human-
473 induced vegetation types, i.e. the reconstructed openland cover can be either natural or human-induced, or both.
474 This issue is discussed thoroughly in Li et al. (2020) as well as the difficulty to infer the occurrence of past crops
475 such as rice and millet from pollen records. Although pollen of cereals such as *Triticum* (wheat), *Hordeum* (barley)
476 and *Zea mays* (corn) can be separated from pollen of wild grasses, a RPP value for these types of cereals could not
477 be estimated in the study of Li et al. (2018b). Moreover, pollen grains from several crops belonging to the families
478 Fabaceae, Brassicaceae, Asteraceae, and Apiaceae cannot be separated from the wild species (Ni et al., 2014). The

479 interpretation of past changes in openland cover needs to take into account the issues described above. This is a
480 limitation of the gridded REVEALS land-cover dataset if used for validation of ALCC scenarios and studies of
481 human-induced land-cover change as a climate forcing. Overestimation of deforestation in ALCCs can be detected
482 in a comparison with REVEALS estimates of past openland, whereas an underestimation cannot be demonstrated
483 (Harrison et al., 2020). This issue is particularly problematic in regions of northern China where steppes, desert,
484 and meadows were dominant over most of the Holocene. Similar limitations exist for the gridded REVEALS land-
485 cover datasets in Europe, although less serious as early agriculture developed primarily on land where woodland
486 was the natural climate-induced vegetation cover and only a smaller fraction of the continent was characterized by
487 steppe vegetation (Trondman et al., 2015; Githumbi et al., 2022; Strandberg et al., 2022).

488 The time resolution of the REVEALS reconstructions (500 years over most of the Holocene) is another limitation
489 in terms of quantification of land-cover change. A relatively low time resolution implies that major but rapid land-
490 cover changes will be missed or underestimated as they will be agglomerated into a mean cover over 500 years.
491 The chosen time resolution is a compromise to improve the quality of the REVEALS estimates by increasing
492 pollen sums for pollen records characterized by a low time resolution of pollen counts (i.e. decrease the standard
493 error of the reconstruction, see methods for more details). Increasing the time resolution would be an advantage
494 only for regions, and periods of the Holocene, for which most pollen records have a high time resolution.

495 Finally, half of the REVEALS reconstructions (18 per time windows) are based on pollen records located within
496 several adjacent $1^\circ \times 1^\circ$ grid cells (a total of 57 $1^\circ \times 1^\circ$ grid cells divided into 18 groups of 2 to 5 grid cells; Figure
497 1) rather than within single $1^\circ \times 1^\circ$ grid cells (18 REVEALS reconstructions per time window). This implies that
498 these 18 REVEALS estimates of cover (covering 57 $1^\circ \times 1^\circ$ grid cells) represent a mean cover for areas of $1^\circ \times 2^\circ$
499 to $1^\circ \times 5^\circ$. The latter can be a limitation if the dataset of past land cover is used for studies in which the variability
500 of plant cover at a $1^\circ \times 1^\circ$ spatial scale is of importance. We opted for this deviation from the standard protocol
501 used in the REVEALS land-cover reconstructions for Europe (Trondman et al., 2015; Githumbi et al., 2022)
502 because of the low spatial density of pollen records in many parts of China and its negative consequence for the
503 quality of the REVEALS reconstructions if they were performed at a $1^\circ \times 1^\circ$ spatial scale implying a too low
504 number of pollen records per grid cell.

505

506 **5. Potential application of the REVEALS estimates**

507 Quantitative reconstruction of land cover at regional to global scales is necessary for the study of climate-land
508 cover interactions using both regional and global climate models, and for evaluation of ALCC scenarios and
509 dynamic vegetation models. This first dataset of REVEALS land cover for temperate and northern subtropical
510 China is a contribution to PAGES LandCover6k, whose purpose was to provide datasets of Holocene pollen-based
511 land cover and archaeology-based land-use useful for (palaeo-) climate modeling (Gaillard et al., 2018; Harrison
512 et al., 2020). Such datasets are an alternative to pollen-based reconstructions of vegetation cover using biomization
513 (Prentice and Webb III, 1998) or the Modern Analog Technique (Overpeck et al., 1985). REVEALS
514 reconstructions have the advantage to provide estimates of cover for individual plant taxa that can be aggregated
515 into cover of groups of taxa such as PFTs or land-cover units. They can be used for various purposes, such as the
516 evaluation of scenarios of past deforestation (HYDE and KK) (Kaplan et al., 2017) or comparison with simulations
517 of past vegetation cover using dynamic vegetation models (Marquer et al., 2014, 2017). For use in climate

518 modeling experiments, looking into e.g. past human-induced land cover (or land use) as a climate forcing, the
519 REVEALS plant-cover data need to be interpolated over all grid cells of the simulation geographical domain using
520 for instance spatial statistics (e.g. Strandberg et al., 2022; see also the Introduction section). Such studies have not
521 been performed in China so far, although comparison of the REVEALS reconstructions of openland, CT and BT
522 cover presented here with HYDE 3.2 and KK10 is in progress (Li et al., in preparation). Further, studies attempting
523 to disentangle the effects of climate and land-use change on plant cover through the Holocene or looking into
524 changes in diversity indices based on REVEALS estimates of past plant cover (e.g. studies by Marquer et al. (2014,
525 2017) in Europe), would also be of great interest in a Chinese context. Another possible use of Holocene
526 REVEALS-estimated of plant cover is the comparison of regional plant-cover change with archaeological data to
527 study the effect of large-scale changes in population growth and settlement patterns and density on vegetation
528 cover in the past. A first attempt at such a comparison in eastern China shows that phases of deforestation as
529 interpreted from the REVEALS estimates of open land cover between 6 and 3 ka BP are well correlated with
530 changes in settlement densities over the same time period, as suggested by archaeological data and population
531 growth based on ¹⁴C dates of archaeological artefacts (Li et al., 2018a)

532

533 6. Data availability

534 All data files are available for public download at the National Tibetan Plateau Data Center (TPDC; Li et al., 2022;
535 <https://data.tpdac.cn/en/disallow/d18d2b7e-25fe-49da-b1bd-2be6014162b0/>). For more details on the files
536 available at the link, see section 2.4 on data format.

537 7. Conclusions

538 This paper describes the first dataset of Holocene gridded pollen-based REVEALS reconstructions of plant taxa at
539 a 1° × 1° spatial scale and continuous temporal scale of 500 years (350, 250, and 100 + x years from 0.7 k BP to
540 1950 CE + x years (x years is the number of years between 1950 CE and the year of coring). The reconstructions
541 are based on 94 pollen records in temperate and northern subtropical China and include land-cover estimates for
542 27 plant taxa and aggregation to plant functional types and three land-cover types. The REVEALS model
543 assumptions and the limitations of this particular application are clearly stated, in order to facilitate a correct and
544 cautious interpretation and assessment of the results. In particular, the consequences of the lack of estimates for
545 the cover of two major conifer trees (*Abies* and *Picea*), bareground, and crop land need to be taken into account in
546 any studies using the dataset, in particular for the vegetation zones II and IV (*Abies*, *Picea*), and VI, VII, and VIII
547 (bareground, crop land). Examples of uses are the evaluation of model-simulated vegetation cover and
548 deforestation from dynamic vegetation models and ALCC scenarios, respectively, as well as studies of past land-
549 use change as climate forcing during the Holocene. In all uses of the presented gridded REVEALS land-cover
550 dataset, the limitations of the REVEALS reconstructions have to be taken into account carefully (see Discussion
551 section for more details). Reconstructions of plant cover at a local spatial scale can be of value in archaeological
552 contexts. One of the input data required for the application of the LOcal Vegetation Estimates model (LOVE;
553 Sugita, 2007b) to estimate local plant cover is that regional plant cover. The dataset of gridded REVEALS
554 reconstructions may be a way to achieve reconstructions of local plant cover, with the condition that the pollen
555 records used for the LOVE application are not used in the REVEALS reconstructions of the dataset (Cui et al.,
556 2013; Mazier et al., 2015).

557 This dataset is the first generation of gridded REVEALS Holocene land-cover reconstructions for China. We
558 expect that, in the future, new generations of such datasets will develop, in which the quality and spatial extent of
559 the REVEALS estimates will be further improved, as more pollen records will be available, and additional RPP
560 studies will gradually increase both the number of RPP values per taxon and the number of taxa for which RPPs
561 are available.

562

563 **Author Contribution**

564 FL and MJG conceptualized and coordinated the study as a contribution to the PAGES working group
565 “LandCover6k”. SS solved all specific issues related to the application of REVEALS in the context of China’s
566 vegetation history and available pollen records. FL, XC, UH, and JN were responsible for collection of new pollen
567 records from individual authors. YZ contributed several published and unpublished pollen records and made
568 comments and edits to the manuscript. JN, CA, XH, YL, HL, AS, YY contributed pollen data. FL had the major
569 responsibility of pollen data files handling, and collection of related metadata, and performed the REVEALS
570 application. FL and MJG are responsible of the paper’s main objective and structure, FL prepared the first draft
571 of the manuscript, all figures and Tables, and finalization of the manuscript for submission. MJG contributed to
572 text in all its versions and checked the final manuscript for content and English language. All co-authors
573 contributed with comments and corrections to the manuscript.

574

575 **Competing interests**

576 The authors declare that they have no conflict of interest.

577

578 **Funds**

579 This work is supported by the National Science Foundation of China (NSCF) (PI Furong Li) [grant number,
580 42101143] and funds from the Swedish Strategical Research Area Modelling the Regional and Global Ecosystem,
581 MERGE (<http://www.merge.lu.se/>) (Furong Li (until 2019) and Marie-José Gaillard). We are also grateful for the
582 financial support from the Swedish Foundation for International Cooperation in Research and Higher Education
583 (STINT) and the NSFC [grant number, 41611130050] for a Sweden-China Exchange Grant 2016–2019 (PIs
584 Marie-José Gaillard). Furong Li (until 2020) and Marie-José Gaillard are grateful for support from the Faculty of
585 Health and Life Sciences at Linnaeus University, Kalmar, Sweden. This study was undertaken as part of the Past
586 Global Changes (PAGES) project and its working group LandCover6k that in turn received support from the Swiss
587 National Science Foundation, the Swiss Academy of Sciences, the US National Science Foundation, and the
588 Chinese Academy of Sciences.

589 **Acknowledgments**

590 We are grateful to all palynologists who either contributed original pollen counts to this work (Bo Cheng, Yaqin
591 Hu, Jie Li, Shicheng Tao, YongBo Wang, Ruilin Wen, and Zhuo Zheng) or to the pollen database published by
592 Cao et al. (2013) from which we used a number of pollen records in this study.

594 **References**

595

596 Cao, X.-y., Ni, J., Herzschuh, U., Wang, Y.-b., and Zhao, Y.: A late Quaternary pollen dataset from eastern
 597 continental Asia for vegetation and climate reconstructions: Set up and evaluation, *Review of Palaeobotany and*
 598 *Palynology*, 194, 21-37, <http://dx.doi.org/10.1016/j.revpalbo.2013.02.003>, 2013.

599 Claussen, M., Bathiany, S., Brovkin, V., & Kleinen, T. (2013). Simulated climate-vegetation interaction in semi-
 600 arid regions affected by plant diversity. *Nature Geoscience*, 6(11), 954–958. <https://doi.org/10.1038/ngeo1962>

601 Cui, Q. Y., Gaillard, M. J., Lemdahl, G., Sugita, S., Greisman, A., Jacobson, G. L., and Olsson, F.: The role of
 602 tree composition in Holocene fire history of the hemiboreal and southern boreal zones of southern Sweden, as
 603 revealed by the application of the Landscape Reconstruction Algorithm: Implications for biodiversity and
 604 climate-change issues, *The Holocene*, 23, 1747-1763, [10.1177/0959683613505339](https://doi.org/10.1177/0959683613505339), 2013.

605 Dawson, A., Cao, X., Chaput, M., Hopla, E., Li, F., Edwards, M., Fyfe, R., Gajewski, K., Goring, S. J.,
 606 Herzschuh, U., Mazier, F., Sugita, S., Williams, J., Xu, Q., and Gaillard, M.-J.: Finding the magnitude of human-
 607 induced Northern Hemisphere land-cover transformation between 6 and 0.2 ka BP, *Past Global Changes*
 608 *Magazine*, 26, 34-35, [10.22498/pages.26.1.34](https://doi.org/10.22498/pages.26.1.34), 2018.

609 Gaillard, M.-J., Morrison, K., Madella, M., and Whitehouse, N.: Past land-use and land-cover change: the
 610 challenge of quantification at the subcontinental to global scales, 3-3 pp., [10.22498/pages.26.1.3](https://doi.org/10.22498/pages.26.1.3), 2018.

611 Gaillard, M.-J., Kleinen, T., Samuelsson, P., Nielsen, A. B., Bergh, J., Kaplan, J., Poska, A., Sandström, C.,
 612 Strandberg, G., Trondman, A.-K., and Wramneby, A.: Causes of Regional Change—Land Cover, in: *Second*
 613 *Assessment of Climate Change for the Baltic Sea Basin*, edited by: The, B. I. I. A. T., Springer International
 614 Publishing, Cham, 453-477, [10.1007/978-3-319-16006-1_25](https://doi.org/10.1007/978-3-319-16006-1_25), 2015.

615 Gaillard, M. J., Sugita, S., Mazier, F., Trondman, A. K., Broström, A., Hickler, T., Kaplan, J. O., Kjellström, E.,
 616 Kokfelt, U., Kuneš, P., Lemmen, C., Miller, P., Olofsson, J., Poska, A., Rundgren, M., Smith, B., Strandberg, G.,
 617 Fyfe, R., Nielsen, A. B., Alenius, T., Balakauskas, L., Barnekow, L., Birks, H. J. B., Bjune, A., Björkman, L.,
 618 Giesecke, T., Hjelle, K., Kalnina, L., Kangur, M., van der Knaap, W. O., Koff, T., Lagerås, P., Latalowa, M.,
 619 Leydet, M., Lechterbeck, J., Lindbladh, M., Odgaard, B., Peglar, S., Segerström, U., von Stedingk, H., and
 620 Seppä, H.: Holocene land-cover reconstructions for studies on land cover-climate feedbacks, *Climate of the Past*,
 621 6, 483-499, [10.5194/cp-6-483-2010](https://doi.org/10.5194/cp-6-483-2010), 2010.

622 ©

623 Harrison, S. P., Gaillard, M. J., Stocker, B. D., Vander Linden, M., Klein Goldewijk, K., Boles, O., Braconnot,
 624 P., Dawson, A., Fluet-Chouinard, E., Kaplan, J. O., Kastner, T., Pausata, F. S. R., Robinson, E., Whitehouse, N.
 625 J., Madella, M., and Morrison, K. D.: Development and testing scenarios for implementing land use and land
 626 cover changes during the Holocene in Earth system model experiments, *Geosci. Model Dev.*, 13, 805-824,
 627 [10.5194/gmd-13-805-2020](https://doi.org/10.5194/gmd-13-805-2020), 2020.

628 Hellman, S., Gaillard, M.-J., Broström, A., and Sugita, S.: The REVEALS model, a new tool to estimate past
 629 regional plant abundance from pollen data in large lakes: validation in southern Sweden, *Journal of Quaternary*
 630 *Science*, 23, 21-42, [10.1002/jqs.1126](https://doi.org/10.1002/jqs.1126), 2008a.

631 Hellman, S. E. V., Gaillard, M.-j., Broström, A., and Sugita, S.: Effects of the sampling design and selection of
 632 parameter values on pollen-based quantitative reconstructions of regional vegetation: a case study in southern
 633 Sweden using the REVEALS model, *Vegetation History and Archaeobotany*, 17, 445-459, [10.1007/s00334-008-](https://doi.org/10.1007/s00334-008-0149-7)
 634 [0149-7](https://doi.org/10.1007/s00334-008-0149-7), 2008b.

635 Hou, X.: 1:1 million vegetation map of China, National Tibetan Plateau Data Center [dataset], 2019.

636 Huntley, B. and Birks, H. J. B.: An atlas of past and present pollen maps for Europe: 0–13,000 years ago. ,
 637 Cambridge: University Press, 1983.

638 Huntley, B. and III., T. W.: HANDBOOK OF VEGETATION SCIENCE, *Vegetation history.* , Cambridge
 639 University Press, 803 pp. 1988.

640 Jackson, S. T., & Lyford, M. E.. Pollen dispersal models in Quaternary plant ecology: Assumptions, parameters,
 641 and prescriptions. *The Botanical Review*, 65(1), 39-75. [doi:10.1007/BF02856557](https://doi.org/10.1007/BF02856557). 1999.

642 Kaplan, J. O., Krumhardt, K. M., and Zimmermann, N.: The prehistoric and preindustrial deforestation of
 643 Europe, *Quaternary Science Reviews*, 28, 3016-3034, <http://dx.doi.org/10.1016/j.quascirev.2009.09.028>, 2009.

644 Kaplan, J. O., Krumhardt, K. M., Gaillard, M. J., Sugita, S., Trondman, A. K., Fyfe, R., Marquer, L., Mazier, F.,
 645 and Nielsen, A. B.: Constraining the Deforestation History of Europe: Evaluation of Historical Land Use
 646 Scenarios with Pollen-Based Land Cover Reconstructions, *Land*, 6, 91, ARTN 91 [10.3390/land6040091](https://doi.org/10.3390/land6040091), 2017.

647 Klein Goldewijk, K., Beusen, A., Doelman, J., and Stehfest, E.: Anthropogenic land use estimates for the
648 Holocene – HYDE 3.2, *Earth Syst. Sci. Data*, 9, 927-953, 10.5194/essd-9-927-2017, 2017.

649 Klein Goldewijk, K., Beusen, A., van Drecht, G., and de Vos, M.: The HYDE 3.1 spatially explicit database of
650 human-induced global land-use change over the past 12,000 years, *Global Ecology and Biogeography*, 20, 73-
651 86, 10.1111/j.1466-8238.2010.00587.x, 2011.

652 Li, F., Cao, X., Herzsuh, U., Jia, X., Sugita, S., Tarasov, P., Wagner, M., Xu, Q., Chen, F., Sun, A., and
653 Gaillard, M.-J.: What do pollen-based quantitative reconstructions of plant cover tell us about past anthropogenic
654 deforestation in eastern china?, *Pages Magazine*, 2018a.

655 Li, F., Gaillard, M.-J., Xu, Q., Bunting, M. J., Li, Y., Li, J., Mu, H., Lu, J., Zhang, P., Zhang, S., Cui, Q., Zhang,
656 Y., and Shen, W.: A Review of Relative Pollen Productivity Estimates From Temperate China for Pollen-Based
657 Quantitative Reconstruction of Past Plant Cover, 9, 10.3389/fpls.2018.01214, 2018b.

658 Li, F., Gaillard, M.-J., Cao, X., Herzsuh, U., Sugita, S., Tarasov, P. E., Wagner, M., Xu, Q., Ni, J., Wang, W.,
659 Zhao, Y., An, C., Beusen, A. H. W., Chen, F., Feng, Z., Goldewijk, C. G. M. K., Huang, X., Li, Y., Li, Y., Liu,
660 H., Sun, A., Yao, Y., Zheng, Z., and Jia, X.: Towards quantification of Holocene anthropogenic land-cover
661 change in temperate China: A review in the light of pollen-based REVEALS reconstructions of regional plant
662 cover, *Earth-Science Reviews*, 103119, <https://doi.org/10.1016/j.earscirev.2020.103119>, 2020.

663 Lu, Z., Miller, P. A., Zhang, Q., Zhang, Q., Wårlind, D., Nieradzik, L., et al. (2018). Dynamic vegetation
664 simulations of the mid-Holocene Green Sahara. *Geophysical Research Letters*, 45. <https://doi.org/10.1029/2018GL079195>

665 Marquer, L., Gaillard, M.-J., Sugita, S., Trondman, A.-K., Mazier, F., Nielsen, A. B., Fyfe, R. M., Odgaard, B.
666 V., Alenius, T., Birks, H. J. B., Bjune, A. E., Christiansen, J., Dodson, J., Edwards, K. J., Giesecke, T.,
667 Herzsuh, U., Kangur, M., Lorenz, S., Poska, A., Schult, M., and Seppä, H.: Holocene changes in vegetation
668 composition in northern Europe: why quantitative pollen-based vegetation reconstructions matter, *Quaternary
669 Science Reviews*, 90, 199-216, <http://dx.doi.org/10.1016/j.quascirev.2014.02.013>, 2014.

671 Marquer, L., Gaillard, M.-J., Sugita, S., Poska, A., Trondman, A.-K., Mazier, F., Nielsen, A. B., Fyfe, R. M.,
672 Jönsson, A. M., Smith, B., Kaplan, J. O., Alenius, T., Birks, H. J. B., Bjune, A. E., Christiansen, J., Dodson, J.,
673 Edwards, K. J., Giesecke, T., Herzsuh, U., Kangur, M., Koff, T., Latałowa, M., Lechterbeck, J., Olofsson, J.,
674 and Seppä, H.: Quantifying the effects of land use and climate on Holocene vegetation in Europe, *Quaternary
675 Science Reviews*, 171, 20-37, <https://doi.org/10.1016/j.quascirev.2017.07.001>, 2017.

676 Mazier, F., Gaillard, M. J., Kuneš, P., Sugita, S., Trondman, A. K., and Broström, A.: Testing the effect of site
677 selection and parameter setting on REVEALS-model estimates of plant abundance using the Czech Quaternary
678 Palynological Database, *Review of Palaeobotany and Palynology*, 187, 38-49,
679 <http://dx.doi.org/10.1016/j.revpalbo.2012.07.017>, 2012.

680 Mazier, F., Broström, A., Bragée, P., Fredh, D., Stenberg, L., Thiere, G., Sugita, S., and Hammarlund, D.: Two
681 hundred years of land-use change in the South Swedish Uplands: comparison of historical map-based estimates
682 with a pollen-based reconstruction using the landscape reconstruction algorithm, *Vegetation History and
683 Archaeobotany*, 24, 555-570, 10.1007/s00334-015-0516-0, 2015.

684 Morrison, K., Gaillard, M. J., Madella, M., Whitehouse, N., and Hammer, E.: Land-use classification, *Past
685 Global Change Magazine*, 24, 40-40, 10.22498/pages.24.1.40, 2016.

686 Ni, J., Cao, X., Jeltsch, F., and Herzsuh, U.: Biome distribution over the last 22,000 yr in China,
687 *Palaeogeography, Palaeoclimatology, Palaeoecology*, 409, 33-47,
688 <http://dx.doi.org/10.1016/j.palaeo.2014.04.023>, 2014.

689 Ni, J., Yu, G., Harrison, S. P., and Prentice, I. C.: Palaeovegetation in China during the late Quaternary: Biome
690 reconstructions based on a global scheme of plant functional types, *Palaeogeography, Palaeoclimatology,
691 Palaeoecology*, 289, 44-61, 10.1016/j.palaeo.2010.02.008, 2010.

692 Overpeck, J. T., Webb III, T., and Prentice, I. C.: Quantitative interpretation of fossil pollen spectra:
693 Dissimilarity coefficients and the method of modern analogs, *Quaternary Research*, 23, 87-108,
694 [http://dx.doi.org/10.1016/0033-5894\(85\)90074-2](http://dx.doi.org/10.1016/0033-5894(85)90074-2), 1985.

695 Prentice, I. C.: Pollen representation, source area, and basin size: Toward a unified theory of pollen analysis,
696 *Quaternary Research*, 23, 76-86, [http://dx.doi.org/10.1016/0033-5894\(85\)90073-0](http://dx.doi.org/10.1016/0033-5894(85)90073-0), 1985.

697 Prentice, I. C. and Webb III, T.: BIOME 6000: reconstructing global mid-Holocene vegetation patterns from
698 palaeoecological records, 25, 997-1005, <https://doi.org/10.1046/j.1365-2699.1998.00235.x>, 1998.

699 Ren, G. and Beug, H.-J.: Mapping Holocene pollen data and vegetation of China, *Quaternary Science Reviews*,
700 21, 1395-1422, [http://dx.doi.org/10.1016/S0277-3791\(01\)00119-6](http://dx.doi.org/10.1016/S0277-3791(01)00119-6), 2002.

701 Ren, G. and Zhang, L.: A preliminary mapped summary of holocene pollen data for northeast China, *Quaternary
702 Science Reviews*, 17, 669-688, [http://dx.doi.org/10.1016/S0277-3791\(98\)00017-1](http://dx.doi.org/10.1016/S0277-3791(98)00017-1), 1998.

703 Strandberg, G., Lindström, J., Poska, A., Zhang, Q., Fyfe, R., Githumbi, E., Kjellström, E., Mazier, F., Nielsen,
704 A., Sugita, S., Trondman, A.-K., Woodbridge, J., and Gaillard, M.-J.: Mid-Holocene European climate revisited:

705 New high-resolution regional climate model simulations using pollen-based land-cover, *Quaternary Science*
706 *Reviews*, 281, 107431, 10.1016/j.quascirev.2022.107431, 2022.

707 Strandberg, G., Kjellström, E., Poska, A., Wagner, S., Gaillard, M. J., Trondman, A. K., Mauri, A., Davis, B. A.
708 S., Kaplan, J. O., Birks, H. J. B., Bjune, A. E., Fyfe, R., Giesecke, T., Kalnina, L., Kangur, M., van der Knaap,
709 W. O., Kokfelt, U., Kuneš, P., Latałowa, M., Marquer, L., Mazier, F., Nielsen, A. B., Smith, B., Seppä, H., and
710 Sugita, S.: Regional climate model simulations for Europe at 6 and 0.2 k BP: sensitivity to changes in
711 anthropogenic deforestation, *Climate of the Past*, 10, 661-680, 10.5194/cp-10-661-2014, 2014.

712 Stuart, A. and Ord, J. K.: *Kendall's Advanced Theory of Statistics. Vol. 1: Distribution Theory*. London:
713 Griffin., 1994.

714 Sugita, S.: Theory of quantitative reconstruction of vegetation I: pollen from large sites REVEALS regional
715 vegetation composition, *The Holocene*, 17, 229-241, 10.1177/0959683607075837, 2007a.

716 Sugita, S.: Theory of quantitative reconstruction of vegetation II: all you need is LOVE, *The Holocene*, 17, 243-
717 257, 10.1177/0959683607075838, 2007b.

718 Sugita, S., Parshall, T., Calcote, R., and Walker, K.: Testing the Landscape Reconstruction Algorithm for
719 spatially explicit reconstruction of vegetation in northern Michigan and Wisconsin, *Quaternary Research*, 74,
720 289-300, 10.1016/j.yqres.2010.07.008, 2010.

721 Sun, Y., Xu, Q., Gaillard, M.-J., Zhang, S., Li, D., Li, M., Li, Y., Li, X., and Xiao, J.: Pollen-based
722 reconstruction of total land-cover change over the Holocene in the temperate steppe region of China: An attempt
723 to quantify the cover of vegetation and bare ground in the past using a novel approach, *CATENA*, 214, 106307,
724 <https://doi.org/10.1016/j.catena.2022.106307>, 2022.

725 Tian, F., Cao, X., Dallmeyer, A., Ni, J., Zhao, Y., Wang, Y., and Herzschuh, U.: Quantitative woody cover
726 reconstructions from eastern continental Asia of the last 22 kyr reveal strong regional peculiarities, *Quaternary*
727 *Science Reviews*, 137, 33-44, <http://dx.doi.org/10.1016/j.quascirev.2016.02.001>, 2016.

728 Trondman, A.-K., Gaillard, M.-J., Sugita, S., Björkman, L., Greisman, A., Hultberg, T., Lagerås, P., Lindbladh,
729 M., and Mazier, F.: Are pollen records from small sites appropriate for REVEALS model-based quantitative
730 reconstructions of past regional vegetation? An empirical test in southern Sweden, *Vegetation History and*
731 *Archaeobotany*, 25, 131-151, 10.1007/s00334-015-0536-9, 2016.

732 Trondman, A. K., Gaillard, M. J., Mazier, F., Sugita, S., Fyfe, R., Nielsen, A. B., Twiddle, C., Barratt, P., Birks,
733 H. J. B., Bjune, A. E., Björkman, L., Broström, A., Caseldine, C., David, R., Dodson, J., Dörfler, W., Fischer, E.,
734 van Geel, B., Giesecke, T., Hultberg, T., Kalnina, L., Kangur, M., van der Knaap, P., Koff, T., Kuneš, P.,
735 Lagerås, P., Latałowa, M., Lechterbeck, J., Leroyer, C., Leydet, M., Lindbladh, M., Marquer, L., Mitchell, F. J.
736 G., Odgaard, B. V., Peglar, S. M., Persson, T., Poska, A., Rösch, M., Seppä, H., Veski, S., and Wick, L.: Pollen-
737 based quantitative reconstructions of Holocene regional vegetation cover (plant-functional types and land-cover
738 types) in Europe suitable for climate modelling, *Global Change Biology*, 21, 676-697, 10.1111/gcb.12737, 2015.

739 Wyser, K., Kjellström, E., Koenigk, T., Martins, H., and Döscher, R.: Warmer climate projections in EC-Earth3-
740 Veg: the role of changes in the greenhouse gas concentrations from CMIP5 to CMIP6, *Environmental Research*
741 *Letters*, 15, 054020, 10.1088/1748-9326/ab81c2, 2020.